polarity. Spin-valve type giant magnetoresistance(SV-GMR) sensors have a maximum resistance change approximately up to 20 % for external magnetic fields and saturation fields are 1.0 – 8.0 mT [1]. SV-GMR sensor has a high sensitivity and a high spatial resolution [2].

Nondestructive evaluation (NDE) is a very broad and interdisciplinary area that can be used to detect defects and measure physical or mechanical characteristics of a material or component. The popularity and acceptance of NDE as a measurement technique is due to the fact that the system or material under test is not harmed or damaged during testing, and thus the integrity of the object under test is retained [3]. There are a range of magnetic sensors developed for NDE such as superconducting quantum interference device (SQUID), inductive coil, fluxgate, hall element, and GMR.

In this paper we report novel applications of GMR sensor in the fields of eddy-current testing (ECT) and medical treatment. For ECT application, the probe based GMR sensor was fabricated. The proposed probe was used to inspect micro defects on printed circuit board (PCB) and to detect micro conducting bead. In the application of medical engineering, a novel GMR probe with needle structure was fabricated to estimate low concentration magnetic fluid and to detect the magnetic field distribution from nervous action.

2 Comparison of Magnetic Sensors

In order to recognize the advantages of GMR, the comparisons between magnetic sensors are shown in Table 1. Compared to the aforementioned sensors that are being used in NDE, the GMR sensor has the advantages of small and very thin structure and high sensitivity under low magnetic fields up to nT. The temperature dependence is 1/20 of hall element [4-6]. The GMR sensor is a resistive device with two terminals which means that it can be utilized by the way of a microstructure and be expanded to an array structure resulting in simple measurements The SV-GMR sensor also has linear characteristics with a little hysteresis for small signal. These favourable qualities make the SV-GMR device suitable for industrial inspection and detection.

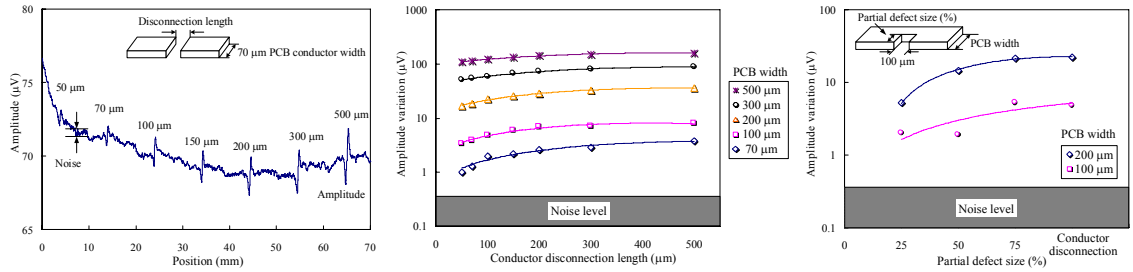

(a) ECT signal obtained from scanning over 70 µm PCB conductor

(b) ECT signal variations against conductor disconnection length

(c) ECT signal variations against partial defects on PCB conductor

Figure 3: Variation of ECT signal on different kinds of defect.

The high frequency ECT probe as shown in Fig. 2 was fabricated for purpose of inspecting micro-crack on a flat surface. The probe includes meander coil as an excitation coil which is fed with high frequency excitation current to provide magnetic fields, and magnetic sensor which will pick up modified magnetic fields B_z due to any defect or boundary on the PCB conductor, that is perpendicular to the scanning direction. When the SV-GMR sensor was mounted between the long meander coils, its sensing axis was set to detect only the magnetic fields B_z. While the long meander coil is primarily used to induce eddy currents on PCB, it also provides the advantage of fabricating a multi-sensor system.

3.2 PCB Conductor Inspection for Detection of Micro Defect [9]

The proposed ECT probe was used for PCB inspection. A PCB model made from copper with a thickness of 9 µm was used for experiment. The PCB conductor had disconnections ranging from 50 to 500 µm.

Fig. 3 (a) shows how the ECT signal varies at defect points and disconnections ranging from 50 - 500 µm can be inspected. Fig. 3(b) shows how the ECT signal variation not only depends on defect size but also on conductor width. Furthermore, it is also possible to inspect partial

Small-signal
haracteristics

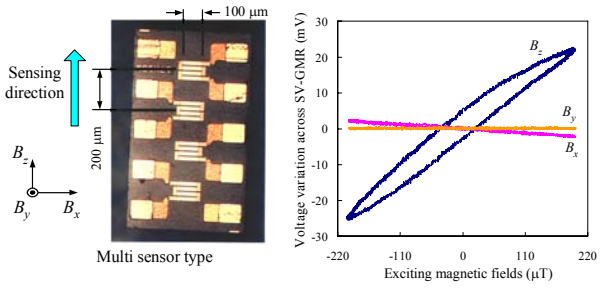

Figure1: Proposed SV-GMR sensor and characteristics.

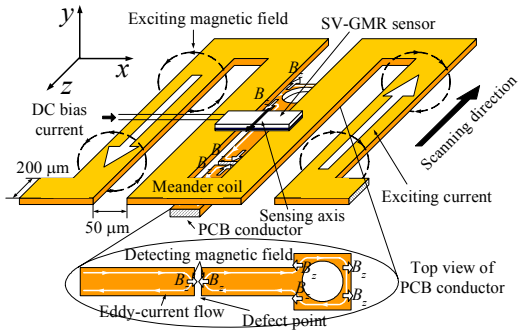

Figure 2: SV-GMR based ECT probe.

Fig. 5 shows the results obtained for detection of conductive microbead. The ECT signal waveforms obtained are for conductive microbead of 125 μm radius at frequency 5 MHz. The results are in good agreement with analytical results. The peak of the ECT signal and signal gradient is used to determine the microbead diameter and its position. Fig. 6 shows the maximum signal variation of the ECT signal for a conductive microbead radius range from 125 to 300 μm. Fig. 7(a) shows the results for determining conductive microbead position. To determine the position of the conductive microbead, the numerical gradient technique is applied to the ECT signal. The pitches of the conductive microbead are also measured by considering the peak of the signal gradient. Figs. 7(b) and (c) show the detection results for microbead array model consisting of microbead of 125 μm radius. The results show that the conductive microbeads can be clearly recognized and the conductive microbead pitch can also be accurately estimated with an error of less than 50 μm. This technique enables the detection of smaller microbead when the SV-GMR sensor is placed as close as possible to the test

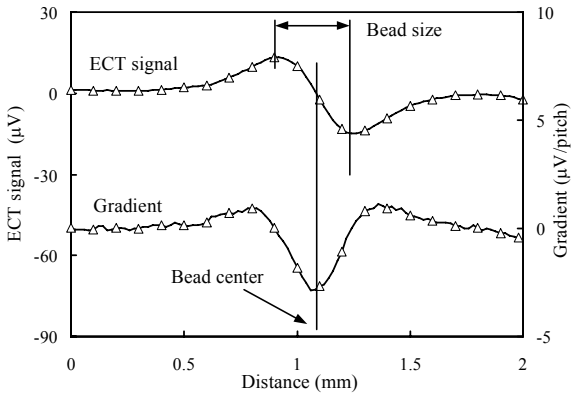

Figure 5: ECT signal obtained from the detection of a conductive microbead (PbSn) with 125 μm radius and its signal gradient.

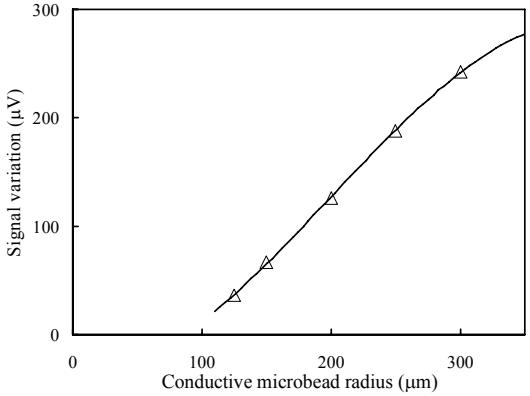

Figure 6: Signal variation vs. microbead(PbSn) radius.

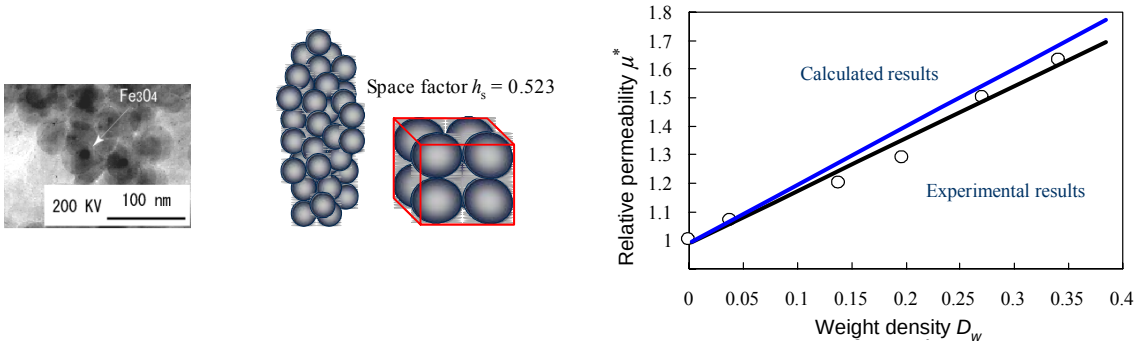

(a) Electron microscopy image and spherical cluster model

(b) Comparison of theoretical and experimental results

Figure 9: Microscopic model of magnetic nanoparticles and relative permeability vs. weight density results.

Sensing direction is parallel to the needle. Constant current of 5 mA is supplied to the GMR sensor. The ac small-signal characteristics at 1 kHz are shown in Fig. 8(b). The sensitivity of the SV-GMR sensor is approximately 12.5 μV/μT.

4.2 Estimation of Magnetic Fluid Weight Density

4.2.1 Magnetic fluid and its applications

The past decade has seen an unprecedented increase in interest for the utilization of magnetic nanoparticles in biomedical applications. Magnetic fluid or dextran magnetite (DM) is a complex of dextran and iron oxide particles. It is not simply a suspension of the two but rather chemically binds to the circumference of iron oxide particles, and is stable as a colloid without aggregation or deposition in various solvents or serum [10].

Since the movement of magnetic nanoparticles can be controlled by external magnetic fields, it is used in targeted drug delivery, where it is possible to carry drugs or medicine to a specific site. Also magnetic nanoparticles react strongly to ac magnetic fields and thus, enabling dynamic methods of cancer therapy such as hyperthermia treatment, or they can also be used as contrasting agents in MRI [11].

Hyperthermia treatment involves magnetic nanoparticles being injected to the tumor area [12, 13]. AC magnetic fields heat up the magnetic nanoparticles and the tissues are heated directly due to hysteresis loss. Induced heat capacity depends on amplitude of magnetic field, exciting frequency and weight density D_w of magnetic fluid [14, 15]. Since the injected magnetic fluid spreads inside the tissue it is critical to estimate the weight density of magnetic fluid inside body before as well as after treatment. The proposed SV-GMR sensor has the potential to be indispensable in this sense.

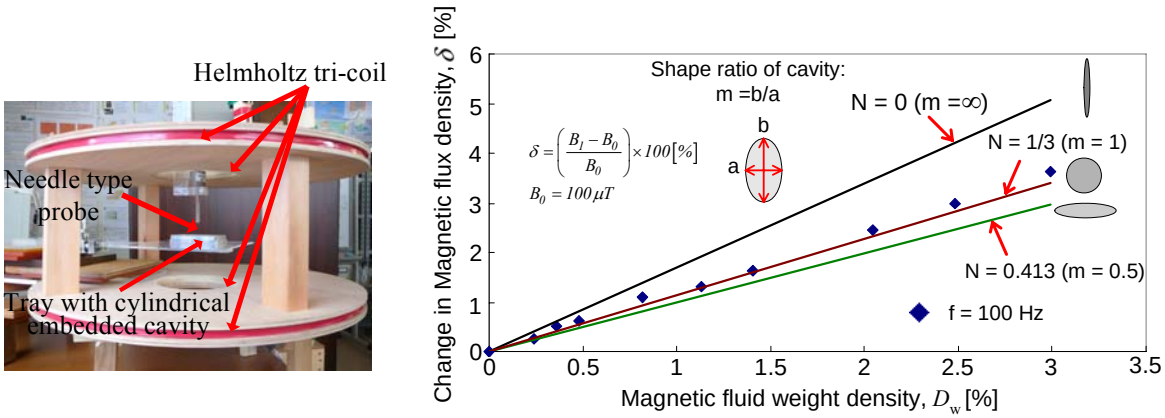

(a) Experimental setup (b) Experimental results

Figure 11: Experimental setup and results for estimation of low concentration magnetic fluid weight density.

calculated from the difference between the applied magnetic flux density, B_0, and the magnetic flux density, B_1, inside the fluid filled cavity. While the change in flux density is proportional to the weight density, the shape of the cavity has an influence on the difference of magnetic flux density.

4.2.3 Dependency of shape ratio and density

Experiments were performed to estimate the low concentration magnetic fluid weight density. The size, shape and composition of magnetic nanoparticles make it an attractive tool in

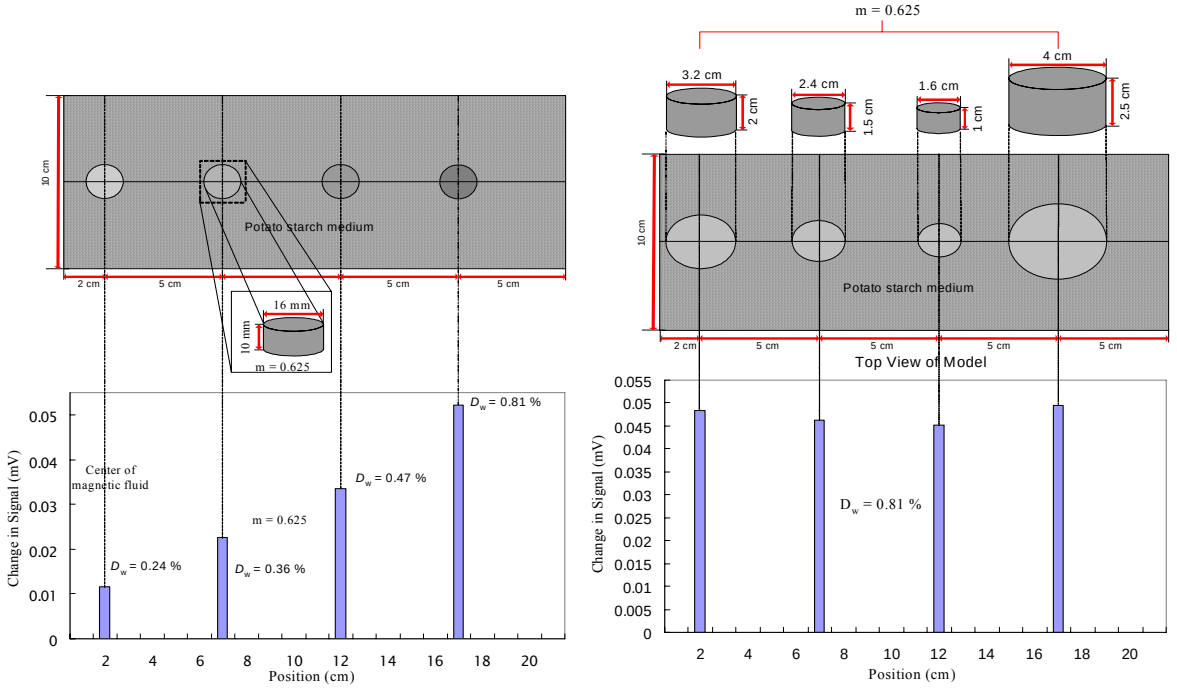

(a) Detection of magnetic fluid of various density (b) Detection of 0.81 % weight density at the shape ratio *m* (height/diameter)=0.625.

Figure 12: Experimental results detecting magnetic fluid weight density.

magnetic fluid filled agar pieces of weight density 0.81 % and different sizes of magnetic fluid filled agar pieces. The different size magnetic fluid filled agar pieces in Fig. 12(b) has m = 0.625 whereas it was m = 1 in Fig. 13. For m = 1, the same diameters and positioning were used as in Fig. 12(b). The results verify Eq. (3) since there does not seem to be a highly significant change in signal between the samples for m = 0.625 and 1.

4.3 Detection of Magnetic Field Distribution from Nervous Action Model

4.3.1 Background and methodology

The detection of magnetic field distribution from nervous action has the potential to diagnose as well as treat neurological diseases. Diseases of the central and peripheral nervous system such as Alzheimer disease, Parkinson disease, and multiple sclerosis are critical for the patient in most cases. Nervous cells in living organisms transmit electrical signals. Signals travel along neurons as waves of electrical discharge at a frequency of around 1 kHz. Action potentials are conducted from dendrites through long axon to other neurons as shown in Fig. 14. The diameter of a typical nerve may vary between 1 and 20 μm [17, 18]. While action impulse travels along the nerve at speeds between 0.6 -120 m/s [19], action current is not more than 1 μA.

Fig. 15 shows the idea of the SV-GMR sensor needle inserted into the proximity of the nerve, and the possible experimental simulation where a magnetic field created around a long thin conductor can be measured, with the sensor placed in the proximity of the wires's lateral surface. Ampere's law is used to calculate the magnetic field distribution in a long thin current carrying wire.

$$B = \mu \frac{I}{2\pi\rho} \qquad (4)$$

where: I ; current flowing in the wire (A),

ρ ; distance from the centre of the wire (m),

μ ; magnetic permeability (H/m),

B ; magnetic flux density (T).

4.3.2 Experimental results

A wire of 15 μm radius was used to simulate a nerve. To simulate action current a pulse signal with 10 % duty cycle at frequency 1 kHz was supplied to the wire. The sensor needle was placed so that it touches the conducting wire. Output signal from the sensor was amplified by

$$\rho = \sqrt{z^2 + r_c^2} \qquad (5)$$

where: z ; vertical height from conductor to point of interest (m),

r_c ; radial distance from conductor (m).

It must be noted that during vertical direction measurements the sensor needle touches the conducting wire as shown in Fig. 17(a) thus making r_c negligible (so ρ is assumed equal to z). However for horizontal measurement as shown in Fig. 17(b), it can be seen that the conducting wire is moved away from the needle, making r_c significant. Fig. 18 compares the experimental results in the vertical direction for 100 μA to the theoretical data. However, it must be noted that we assume the sensor as a point in the theoretical calculation, but in reality it comprises of four thin elements amounting to 40 μm.

A possible reason for the signal in the detecting region not being uniform is that during experiments the positioning of sensor could have introduced some error. Fig. 19 shows the results obtained when the nerve was moved in the horizontal direction until no signal could be deciphered. From the results, it can be seen that the signal can be detected around 750 μm in the horizontal direction from the needle.

Further measurements were performed to simulate measurements through body tissue. Measurements were taken through polyimide layers of differing thickness for 1.0 mA of action current. The results in Fig. 20 show that the detected signal is inversely proportional with increasing layer thickness of polyimide. In neurological measurements, the signals of interest are usually less than microamperes. Fig. 21 shows the signal obtained from the SV-GMR sensor for input currents ranging from 10 μA to 100 nA.

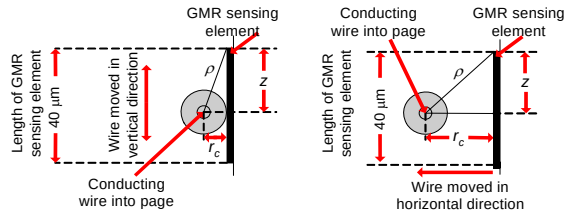

(a) Vertical direction measurement set up

(b) Horizontal direction measurement set up

Figure 17: Measurement of magnetic field in the horizontal and vertical directions.

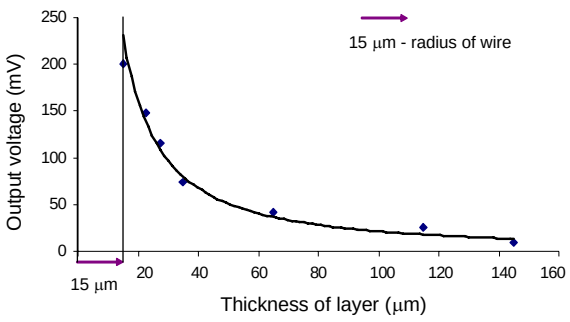

Figure 20: Output voltage versus thickness of polyimide layers placed between conducting wire and sensor at 1.0 mA.

[8] K.Chomsuwan, S.Yamada, M.Iwahara, H. Wakiwaka, S.Shoji, "PCB Conductor Dimension and Alignment Inspection Using an ECT Probe with an SV-GMR Sensor," Transactions on Magnetics Society in Japan, no.5, pp.93-96, 2005.

[9] S.Yamada, K.Chomsuwan, T.Hagino, K. Minamide, M.Iwahara, "Conductive Microbead Array Detection by High-Frequency Eddy-Current Testing Technique," IEEE Transaction on Magnetics, vol.41, no.10, pp.3622-3624, 2005.

[10] I.Nagano, H.Nagae, S.Shiozaki, I.Kawajiri, S. Ygitani, K.Katayama, K. Tazawa, "Development of a Portable Cancer Treatment System Using Induction Heating: a New Weapon for Killing the Cancer," 2nd Kanazawa workshop, pp.11-15, 2006.

[11] G.Reiss, A.Hütten, "Magnetic Nanoparticles: Applications Beyond Data Storage", Nature Materials, vol.4, issue 10, pp.725-726, 2005.

[12] J. van der Zee "Heating the Patient: a Promising Approach?," Annals of Oncology, 13(8), pp. 1173-84, 2002.

[13] R.Hergt, W.Andra, C.G.d'Ambly, I.Hilger, W.A. Kaiser, U.Richter, H.G.Schmidt,"Physical Limits of Hyperthermia Using Magnetic Fine Particles," IEEE Transactions on Magnetics, vol.34, no.5, pp.3745-3754, 1998.

[14] S.Yamada, K.Chomsuwan, S.C.Mukhopadhyay, M.Iwahara, M.Kakikawa, I.Nagano, "Detection of Magnetic Fluid Volume Density With SV-GMR Sensor," Journal of the Magnetics Society of Japan, vol. 31, no. 2, pp. 44-47, 2007.

[15] S.C.Mukhopadhyay, K.Chomsuwan, C.P. Gooneratne, S.Yamada, "A Novel Needle-type SV-GMR Sensor for Bio-Medical Applications," IEEE Sensors Journal, vol. 7, issue. 3, pp. 401-408, 2007.

[16] R.M.Bozorth, Ferromagnetism, 3rd ed, vol.2, Oxford: Clarendon, pp. 845-873, 1989.

[17] J.P.Wikswo, J.P.Barach, J.A.Freeman,"Magnetic Field of a Nerve Impulse: First Measurements", Science, vol.208, issue 4439, pp. 53-55, 1980.

[18] K.R. Swinney, J.P. Wikswo Jr, "A Calculation of the Magnetic Field of a Nerve Action Potential," Biophysical Journal, vol.32, pp.719-731, 1980.

[19] E.Tkacz, P.Borys, Bionika, WNT, pp.41-47, 2006.